Biogeosciences
Discussions

Open Access

EGU

1 **Individual and interactive effects of warming and CO_2 on *Pseudo-nitzschia subcurvata* and**

2 ***Phaeocystis antarctica*, two dominant phytoplankton from the Ross Sea, Antarctica**

3 Zhi Zhu[1], Pingping Qu[1], Jasmine Gale[1], Feixue Fu[1], David A. Hutchins[1]

4 1. Department of Biological Science, University of Southern California, Los Angeles, CA 90089,

5 USA.

6 Correspondence to: David A. Hutchins (dahutch@usc.edu)

7
8 **Abstract:** We investigated the effects of temperature and CO_2 variation on the growth and

9 elemental composition of cultures of the diatom *Pseudo-nitzschia subcurvata* and the

10 prymnesiophyte *Phaeocystis antarctica,* two ecologically dominant phytoplankton species

11 isolated from the Ross Sea, Antarctica. To obtain thermal functional response curves, cultures

12 were grown across a range of temperatures from 0^oC to 14^oC. In addition, a competition

13 experiment examined the relative abundance of both species at 0^oC and 6^oC. CO_2 functional

14 response curves were conducted from 100 to 1730 ppm at 2^oC and 8^oC to test for interactive

15 effects between the two variables. The growth of both phytoplankton was significantly affected

16 by temperature increase, but with different trends. Growth rates of *P. subcurvata* increased with

17 temperature from 0°C to maximum levels at 8°C, while the growth rates of *P. antarctica* only

18 increased from 0°C to 2°C. The maximum thermal limits of *P. subcurvata* and *P. antarctica*

19 where growth stopped completely were 14°C and 10°C, respectively. Although *P. subcurvata*

20 outcompeted *P. antarctica* at both temperatures in the competition experiment, this happened

21 much faster at 6°C than at 0°C. For *P. subcurvata,* there was a significant interactive effect in

22 which the warmer temperature decreased the CO_2 half saturation constant for growth, but this

23 was not the case for *P. antarctica*. The growth rates of both species increased with CO_2 increases

24 up 425 ppm, and in contrast to significant effects of temperature, the effects of CO_2 increase on

25 their elemental composition were minimal. Our results suggest that future warming may be more

26 favorable to the diatom than to the prymnesiophyte, while CO_2 increases may not be a major

27 factor in future competitive interactions between *Pseudo-nitzschia subcurvata* and *Phaeocystis*

28 *antarctica* in the Ross Sea.

Biogeosciences
Discussions

Open Access

EGU

29
30   **1 Introduction**

31   Global temperature is predicted to increase 2.6°C to 4.8°C by 2100 with increasing

32   anthropogenic CO_2 emissions (IPCC, 2014). The temperature of the Southern Ocean has

33   increased even faster than global average temperature (Gille, 2002), and predicted future climate

34   warming may profoundly change the ocean carbon cycle in this region (Sarmiento et al., 1998).

35   The Ross Sea, Antarctica, is one of the most productive area in the ocean, and features annual

36   austral spring and summer algal blooms dominated by *Phaeocystis* and diatoms that contribute as

37   much as 30% of total primary production in the Southern Ocean (Arrigo et al., 1999, 2008;

38   Smith et al., 2000). The response of phytoplankton in the Southern Ocean to future temperature

39   change may offset the decrease of carbon export caused by intensified stratification (Sarmiento

40   et al., 1998), and the physiological effects of warming may partially compensate for a lack of

41   iron throughout much of this region (Hutchins and Boyd, 2016).

42   In the Ross Sea, the colonial prymnesiophyte *Phaeocystis antarctica* typically blooms in

43   austral spring and early summer, and diatoms including *Pseudo-nitzschia subcurvata* and

44   *Chaetoceros* spp. bloom later in the austral summer (Arrigo et al., 1999, 2000; DiTullio and

45   Smith, 1996; Goffart et al., 2000; Rose et al., 2009). Both diatoms and *P. antarctica* play an

46   important role in anthropogenic CO_2 drawdown and the global carbon cycle; additionally, they

47   contribute significantly to the global silicon and sulfur cycles, respectively (Arrigo et al., 1999;

48   Tréguer et al., 1995; Schoemann et al., 2005). Furthermore, the elemental ratios of *P. antarctica*

49   and diatoms are different and thus they contribute unequally to the carbon, nitrogen, and

50   phosphorus cycles (Arrigo et al., 1999, 2000). Diatoms are preferred by zooplankton grazers

51   over *P. antarctica,* and so the two groups also differentially influence the food webs of the

52   Southern Ocean (Knox, 1994; Caron et al., 2000).

53   Arrigo et al. (1999) suggested that the spatial and temporal distributions of *P. antarctica*

54   and diatoms in the Ross Sea are determined by the mixed layer depth, while Liu and Smith

55   (2012) indicated that temperature is more important in shaping the distribution of these two

56   dominant groups of phytoplankton. Zhu et al. (2016) observed that a 4ºC temperature increase

Biogeosciences
Discussions

Open Access

EGU

57   promoted the growth rates of several dominant diatoms isolated from Ross Sea, including *P.*

58   *subcurvata*, *Chaetoceros* sp., and *Fragilariopsis cylindrus*, but not the growth rates of *P.*

59   *antarctica*. In addition, both field and laboratory research has suggested that temperature

60   increase and iron addition can synergistically promote the growth of Ross Sea diatoms (Rose et

61   al., 2009; Zhu et al., 2016; Hutchins and Boyd, 2016). Thus, it is possible that phytoplankton

62   community structure in the Southern Ocean may change in the future under a global warming

63   scenario.

64   In addition to temperature increases, ocean uptake of 30% of total emitted anthropogenic

65   CO_2 has led to a 0.1 pH unit decrease in surface water, corresponding to a 26% increase in

66   acidity (IPCC, 2014). The global CO_2 concentration is predicted to increase to around 800 ppm

67   by 2100, which will lead to a further decrease in surface seawater pH of 0.3–0.4 units (Orr et al.,

68   2005; IPCC, 2014). CO_2 increases have been found to promote the growth and affect the

69   physiology of many but not all phytoplankton species tested (Fu et al., 2007, 2008; King et al.,

70   2011; Xu et al., 2014).

71   Research on the effects of CO_2 increases on *Phaeocystis antarctica* and Antarctic diatoms

72   is still scarce. Xu et al. (2014) suggested that future conditions (higher temperature, CO_2, and

73   light intensity) may shift phytoplankton community structure towards diatoms and away from *P.*

74   *antarctica* in the Ross Sea. Trimborn et al. (2013) discovered that the growth rates of *P.*

75   *antarctica* and *P. subcurvata* were not significantly promoted by high CO_2 relative to ambient

76   CO_2 at 3°C. In contrast, Wang et al. (2010) observed that the growth rates of the closely related

77   temperate colonial species *Phaeocystis globosa* increased significantly at 750 ppm CO_2 relative

78   to 380 ppm CO_2.

79   Thus, an important goal of phytoplankton research is to understand how global warming

80   together with ocean acidification may shift the phytoplankton community in the Southern Ocean

81   (Arrigo et al., 1999; DiTullio et al., 2000). This study aimed to explore the effects of increases in

82   temperature and CO_2 availability, both individually and in combination, on *P. antarctica* and *P.*

83   *subcurvata* isolated from the Ross Sea, Antarctica. These results may shed light on the potential

84 effects of global change on the marine ecosystem and the cycles of carbon and nutrients in the

85 highly productive coastal polynyas of Antarctica.

86
87 **2 Materials and Methods**

88 **2.1 Strains and growth conditions**

89 *P. subcurvata* and *P. antarctica* were isolated from the ice edge in McMurdo Sound (77.62° S,

90 165.47° E) in the Ross Sea, Antarctica during January 2015. All stock cultures were grown in

91 Aquil* medium (100 µmol L^{-1} NO_3^-, 100 µmol L^{-1} SiO_4^{4-}, 10 µmol L^{-1} PO_4^{3-}) made with 0.2 µM-

92 filtered seawater that was collected from the same Ross Sea locale as the culture isolates (Sunda

93 et al., 2005). Because stock and experimental cultures were grown in Fe-replete Aquil medium

94 (0.5 µM), culture conditions most closely resembled the McMurdo Sound ice edge environment

95 in the early spring when Fe is not limiting, prior to being drawn down over the course of the

96 seasonal algal bloom (Bertrand et al., 2015). Cultures were maintained at 0°C in a walk-in

97 incubator under 24 h cold white fluorescence light (80 µmol photons m^{-2} s^{-1}).

98 **2.2 Experimental design**

99 For thermal functional response curves, experimental cultures of both phytoplankton were grown

100 in triplicate 500 ml acid washed polycarbonate bottles and gradually acclimated by a series of

101 step-wise transfers to a range of temperatures, including 0°C, 2°C, 4°C, 6°C, 8°C, and 10°C (*P.*

102 *antarctica* died at 10°C) under the same light cycle as stock cultures. Cultures were diluted semi-

103 continuously following Zhu et al. (2016). All of the cultures were acclimated to their respective

104 temperatures for 8 weeks before the commencement of the experiment. At this point, after the

105 growth rates were verified to be stable for at least three to five consecutive transfers, the cultures

106 were sampled 48 h after dilution (Zhu et al., 2016).

107 For CO_2 functional response curves, *P. antarctica* and *P. subcurvata* were also grown in

108 triplicate in a series of six CO_2 concentrations from ~100 ppm to ~1730 ppm in triplicate 500 ml

109 acid washed polycarbonate bottles at both 2°C and 8°C using same dilution technique as above.

110 The CO_2 concentration was achieved by gently bubbling with 0.2 µm filtered air/CO_2 mixture

111   (Gilmore, CA) and carbonate system equilibration was ensured by pH and dissolved inorganic

112   carbon (DIC) measurements (King et al., 2015, see below).

113   To examine thermal effects on competition between the two species, *P. antarctica* and *P.*

114   *subcurvata* (pre-acclimated to respective temperatures) were mixed at equal Chl *a* (chlorophyll

115   *a*) concentrations and grown together for 6 days in triplicate bottles at both 0°C and 6°C. The

116   relative abundance of each phytoplankton was then calculated based on cell counts taken on days

117   0, 3 and 6.

118   **2.3 Growth rates**

119   Cell count samples were counted on a Sedgewick Rafter Grid using an Olympus BX51

120   microscope before and after dilution for each treatment. Samples that couldn't be counted

121   immediately were preserved with Lugol's (final concentration 2%) and stored at 4°C until

122   counting. Specific growth rates (d^{-1}) were calculated following Eq. (1):

123    $\mu = (\ln N_1 - \ln N_0)/t$,   (1)

124   where N_0 and N_1 are the cell density at the beginning and end of a dilution period, respectively,

125   and t is the duration of the dilution period (Zhu et al. 2016). The Q_{10} of growth rates was

126   calculated following Chaui-Berlinck et al. (2002) as Eq. (2):

127    $Q_{10} = (\mu_2/ \mu_1)^{10/(T_2 - T_1)}$,   (2)

128   where μ_1 and μ_2 are the specific growth rates of the phytoplankton at temperatures T_1 and T_2,

129   respectively. The growth rates were fitted to Eq. (3) to estimate the thermal reaction norms of

130   each species:

131    $f(T) = a e^{bT}(1- ((T-z)/(w/2))^2)$,   (3)

132   where specific growth rate f depends on temperature (T), temperature niche width (w), and other

133   empirical parameters z, a, and b were estimated by maximum likelihood (Thomas et al., 2012;

134   Boyd et al., 2013). Afterwards, the optimum temperature for growth and maximum growth rate

135   were estimated by numerically maximizing the equation (Boyd et al., 2013). The growth rates of

136   all the species at all the CO_2 levels were fitted to Michaelis-Menten equation as Eq. (4):

137    $\mu = \mu_{max} S/(K_m + S)$,   (4)

138   to estimate maximum growth rates (μ_{max}) and half saturation constants (K_m) for CO_2

139   concentration (S).

2.4 Elemental and Chl *a* analysis

141   Culture samples for particulate organic carbon/nitrogen (POC/PON) and particulate organic

142   phosphorus (POP) analyses were filtered onto pre-combusted (500°C for 2 h) GF/F filters and

143   dried at 60°C overnight. A 30 ml aliquot of *P. subcurvata* culture samples for each treatment

144   were filtered onto 2 μm polycarbonate filters (GE Healthcare, CA) and dried in a 60°C oven

145   overnight for biogenic silica (BSi) analysis. The analysis method of POC/PON and POP

146   followed Fu et al. (2007), and BSi analysis followed Paasche et al. (1973). An aliquot of 30 to 50

147   ml from each treatment replicate was filtered onto GF/F filters and extracted with 90% acetone at

148   -20°C for 24 h for Chl *a* analysis. The Chl *a* concentration was then determined using the non-

149   acidification method on a 10-AU[TM] fluorometer (Turner Design, CA) (Fu et al., 2007).

2.5 pH and dissolved inorganic carbon (DIC) measurements

151   pH was measured using a pH meter (Thermo Scientific, MA), calibrated with pH 7 and 10 buffer

152   solutions. For DIC analyses, an aliquot of 25 mL was preserved with 200 μL 5% $HgCl_2$ and

153   stored in the dark at 4°C until analysis. Total DIC was measured using CM140 Total Inorganic

154   Carbon Analyzer (UIC Inc., IL). An aliquot of 5 mL sample was injected into the sparging

155   column of Acidification Unit CM5230 (UIC Inc., IL) followed by 2 ml 10% phosphoric acid. By

156   using flow rates controlled pure nitrogen as carrier gas, the CO_2 released from the DIC pool in

157   the sample was quantified by CM5015 CO_2 Coulometer (UIC Inc., IL) using absolute

158   coulometric titration. The carbonate buffer system was sampled for each of the triplicate bottles

159   in each treatment at the beginning and end of the experiments; reported values are final ones.

160   The pCO_2 in growth media was calculated using CO2SYS (Pierrot et al., 2006). These carbonate

161   system measurements are shown in Table 1, along with the corresponding calculated pCO_2

162   values calculated. Kinetic parameters were calculated using the individual calculated pCO_2

163   values for each replicate (see above), but for convenience, the CO_2 treatments are referred to in

164   the text using the mean value of all experimental bottles, rounded to the nearest 5 ppm: these

165   values are 100 ppm, 205 ppm, 260 ppm, 425 ppm, 755 ppm, and 1730 ppm.

166   **2.6 Statistical analysis**

167   All statistical analyses and model fitting, including student t-tests, ANOVA, Tukey's HSD test,

168   two-way ANOVA, and thermal reaction norms estimation were conducted using the open source

169   statistical software R version 3.1.2 (R Foundation).

170   **3 Results**

171   **3.1 Temperature effects on growth rates**

172   Temperature increase significantly affected the growth rates of both *P. antarctica* and *P.*

173   *subcurvata*, but with different trends ($p < 0.05$) (Fig. 1). The specific growth rates of *P.*

174   *subcurvata* increased from 0°C to 8°C ($p < 0.05$), and then significantly decreased at 10°C ($p <$

175   0.05) (Fig. 1). The growth rates of *P. antarctica* significantly increased from 0°C to 2°C, and

176   plateaued at 4°C and 6°C, and then significantly decreased from 6°C to 8°C ($p < 0.05$) (Fig. 1).

177   *P. antarctica* and *P. subcurvata* stopped growing at 10°C and 14°C, respectively (Fig. 1A). The

178   specific growth rates of *P. subcurvata* were not significantly different from those of *P. antarctica*

179   at 0°C, 2°C and 4°C, but became significantly higher than *P. antarctica* at 6°C, and remained

180   significantly higher than *P. antarctica* through 8°C and 10°C ($p < 0.05$) (Fig. 1A). The optimum

181   temperatures for growth of *P. antarctica* and *P. subcurvata* were 4.85°C and 7.36°C,

182   respectively (Table 2). In addition, the estimated temperature niche width of *P. subcurvata*

183   (-2°C – 12.19°C) is wider than that of *P. antarctica* (-2.0°C to 9.52°C) (Table 2); calculated

184   minimum temperatures estimated from the thermal niche width equation were less than -2.0°, the

185   freezing point of seawater, and so growth is assumed to terminate at -2.0°. The Q10 value of the

186   growth rate of *P. antarctica* from 0°C to 4°C is 2.11, which is lower than the Q10 values 3.17 for

187   *P. subcurvata* over the same temperature interval ($p < 0.05$) (Table 2).

188   **3.2 Temperature effects on elemental composition**

189   The C:N and N: P ratios of *P. subcurvata* were unaffected by changing temperature (Fig.

190   2A, B), but the C: P, C: Si, and C: Chl *a* ratios of this species were significantly affected ($p <$

191 0.05) (Fig. 2C, D, Fig. 3). The C: P ratios of *P. subcurvata* were slightly but significantly lower

192 in the middle of the tested temperature range. They were higher at 8°C and 10°C than at 2°C,

193 4°C, and 6°C (p < 0.05) (Fig. 2C), and also significantly higher at 10°C than at 0°C (Fig. 2C).

194 The C: Si ratios of *P. subcurvata* showed a similar pattern of slightly lower values at mid-range

195 temperatures; at 0°C and 2°C they were significantly higher than at 6°C and 8°C (p < 0.05) (Fig.

196 2D), and significantly higher at 2°C and 10°C than at 4°C and 8°C, respectively (Fig. 2D). The

197 C: Chl *a* ratios of *P. subcurvata* also showed this trend of somewhat lower values in the middle

198 of the thermal gradient. At 0°C, 8°C and 10°C, C: Chl *a* ratios were significantly higher than at

199 2°C, 4°C, and 6°C (p < 0.05), and also significantly higher at 10°C than at 0°C and 8°C (Fig. 3).

200   The C: N, N: P, C: P, and C: Chl *a* ratios of *P. antarctica* were not significantly different

201 across the temperature range (Fig. 2A, B, C, Fig. 3). The N: P ratios of *P. antarctica* were

202 significantly higher than those of *P. subcurvata* at 2°C, 6°C, and 8°C (p < 0.05) (Fig. 2B).

203 Additionally, the C: P ratios of *P. antarctica* were significantly higher than those of *P.*

204 *subcurvata* at 6°C and 8°C (p < 0.05) (Fig. 2C), and the C: Chl *a* ratios of *P. antarctica* were

205 significantly higher than values of *P. subcurvata* at all the temperatures tested (p < 0.05) (Fig. 3).

206   Temperature change significantly affected the cellular carbon (C) quotas, cellular

207 nitrogen (N) quotas, cellular phosphorus (P) quotas, cellular silica (Si) quotas, and cellular Chl *a*

208 quotas of *P. subcurvata* (p < 0.05) (Table 3). The cellular C and N quotas of *P. subcurvata* were

209 significantly higher at 8°C than at 0°C (p < 0.05) (Table 3), the cellular P quotas of *P.*

210 *subcurvata* were significantly higher at 4°C than at 0°C, 2°C, and 10°C (p < 0.05) (Table 3), and

211 the cellular Si quotas of *P. subcurvata* were significantly higher at 8°C than at 0°C and 2°C. Si

212 quotas were also significantly higher at 4°C and 6°C than at 0°C (p < 0.05) (Table 3). The

213 extreme temperatures significantly decreased the cellular Chl *a* quotas of *P. subcurvata*, as the

214 cellular Chl *a* quotas of this species were significantly higher at 4°C, 6°C, and 8°C than at 0°C

215 and 10°C (p < 0.05) (Table 3).

216   Temperature change significantly affected the cellular P quotas and cellular Chl *a* quotas

217 of *P. antarctica* (p < 0.05), but not the cellular C and N quotas (p > 0.05) (Table 3). The cellular

218   P quotas of *P. antarctica* were significantly higher at 0°C than at 8°C ($p < 0.05$) (Table 3), and

219   the Chl *a* quotas of the prymnesiophyte were significantly lower at 8°C than at 0°C, 2°C, and

220   6°C ($p < 0.05$) (Table 3).

221   3.3 Competition at two temperatures

222   A warmer temperature favored the dominance of *P. ubcurvata* over *P. antarctica* in the

223   competition experiment. Although *P. subcurvata* increased its abundance relative to the

224   prymnesiophyte at both temperatures by day 6, this increase was larger and happened much

225   faster at 6°C (from 31% to 72%) relative to 0°C (from 31% to 38%) ($p < 0.05$) (Fig. 4).

226   3.4 CO_2 effects on specific growth rates at two temperatures

227   The carbonate system was relatively stable across the range of CO_2 levels during the

228   course of the experiment (Table 1). CO_2 concentration significantly affected the growth rates of

229   *P. subcurvata* at both temperatures. The growth rates of the diatom at 2°C increased steadily

230   with CO_2 concentration increase from 205 ppm to 425 ppm ($p < 0.05$), but were saturated at at

231   755 ppm and 1730 ppm (Fig. 5A). Similarly, the growth rates of *P. subcurvata* at 8°C increased

232   with CO_2 concentration increase from 205 ppm to 260 ppm ($p < 0.05$), and were saturated at 425

233   ppm, 755 ppm and 1730 ppm (Fig. 5B). The growth rates of the diatom at all CO_2 concentrations

234   tested at 8°C were significantly higher than at 2°C ($p < 0.05$); for instance, the maximum growth

235   rate of *P. subcurvata* at 8°C was 0.88 d^{-1}, significantly higher than the value of 0.60 d^{-1} at 2°C (p

236    $< 0.0.5$) (Table 4). In addition, the pCO_2 half saturation constant (K_m) of *P. subcurvata* at 8°C

237   was 10.7 ppm, significantly lower than 66.0 ppm at 2°C ($p < 0.0.5$) (Table 4). Thus,

238   temperature and CO_2 concentration increase interactively increased the growth rates of *P.*

239   *subcurvata* ($p < 0.05$).

240   CO_2 concentration also significantly affected the growth rates of *P. antarctica*

241   at both 2°C and 8°C. The growth rates of the prymnesiophyte at both 2°C and 8°C increased with

242   CO_2 concentration increase from 100 ppm to 260 ppm ($p < 0.05$), and were saturated at 425 ppm

243   and 755 ppm (Fig. 5C, D). The growth rates of *P. antarctica* at 2°C decreased slightly at 1730

244   ppm relative to 425 ppm and 755 ppm ($p < 0.05$) (Fig. 5C). The maximum growth rate of *P.*

245 *antarctica* at 8°C was 0.43 d^{-1}, significantly lower than the value of 0.61 d^{-1} at 2°C (p < 0.05) (

246 Table 4). The pCO$_2$ half saturation constants of *P. antarctica* at 2°C and 8°C were not

247 significantly different (Table 4), and thus no interactive effect of temperature and CO$_2$ was

248 observed on the growth rate of the prymnesiophyte (p > 0.05).

249 **3.5 CO$_2$ effects on elemental composition at two temperatures**

250 CO$_2$ concentration variation didn't affect the C: N, N: P, or C: P ratios of *P. subcurvata* at

251 either 2°C or 8°C. The C: Si ratios of *P. subcurvata* were significantly higher at 1730 ppm

252 relative to lower pCO$_2$ levels, except at 755 ppm at 8°C (p < 0.05) (Table 5). The N: P ratios of

253 *P. subcurvata* at 8°C were significantly higher than at 2°C at all the CO$_2$ levels tested except 100

254 ppm (p < 0.05) (Table 5). The C: P ratios of *P. subcurvata* at 8°C were significantly higher than

255 at 2°C at all the CO$_2$ levels tested (p < 0.05) (Table 5). The C: Si ratios of *P. subcurvata* at CO$_2$

256 levels lower than 755 ppm at 8°C were significantly lower than at 2°C (p < 0.05) (Table 5). The

257 higher temperature also significantly increased the C: Chl *a* ratios of *P. subcurvata* at all the CO$_2$

258 levels tested (p < 0.05) (Table 5). Additionally, the temperature increase and CO$_2$ concentration

259 increase interactively decreased the C: Chl *a* ratios of *P. subcurvata* (p < 0.05) (Table 5).

260 The CO$_2$ concentration increase did not affect the C: N, N: P, and C: P ratios of *P.*

261 *antarctica* at either 2°C or 8°C. The carbon to Chl *a* ratios of *P. antarctica* were significantly

262 higher at 1730 ppm than at all lower CO$_2$ concentrations at 2°C. Similarly, at 8°C the carbon to

263 Chl *a* ratios of this species also were significantly higher at 425 ppm, 755 ppm, and 1730 ppm

264 than at lower CO$_2$ concentrations (p < 0.05) (Table 5), and significantly higher at 1730 ppm than

265 at 425 ppm and 755 ppm (p < 0.05) (Table 5).

266 The warmer temperature significantly decreased the C: N ratios of *P. antarctica* at 260

267 ppm and 755 ppm CO$_2$ (p < 0.05) (Table 5), and C: P ratios also decreased at 100 ppm and 205

268 ppm(p < 0.05) (Table 5). The C: Chl *a* ratios of *P. antarctica* at CO$_2$ levels higher than 205 ppm

269 were significantly higher at 8°C relative to 2°C (p < 0.05) (Table 5). Temperature and CO$_2$

270 concentration increase interactively increased the C: Chl *a* ratios of *P. antarctica* (p < 0.05)

271 (Table 5).

Biogeosciences
Discussions

Open Access

EGU

272   The CO_2 concentration increase didn't affect the cellular C, N, P, or Si quotas of *P.*

273   *subcurvata* at 2°C, or the C quotas and N quotas at 8°C. The Si quotas of *P. subcurvata* were

274   significantly lower at 1730 ppm CO_2 than at 100 ppm and 205 ppm at 8°C ($p < 0.05$) (Table 6).

275   The cellular Chl *a* quotas of *P. subcurvata* were significantly lower at 8°C relative to 2°C at CO_2

276   higher than 205 ppm ($p < 0.05$) (Table 6). The temperature increase significantly increased the

277   cellular Si quota of *P. subcurvata* at all the CO_2 levels tested except 1730 ppm ($p < 0.05$) (Table

278   6). Additionally, warming and CO_2 concentration interactively decreased the cellular Si quotas of

279   *P. subcurvata* ($p < 0.05$) (Table 6).

280   The C, N, and P quotas of *P. antarctica* were not affected by CO_2 increase at 2°C, and N

281   and P quotas were not affected by CO_2 increase at 8°C, either. However, the C quota of *P.*

282   *antarctica* at 1730 ppm CO_2 was significantly higher than CO_2 levels lower than 755 ppm at 8°C

283   ($p < 0.05$) (Table 6). The Chl *a* per cell of *P. antarctica* at 1730 ppm CO_2 was significantly less

284   than at lower CO_2 levels at both 2°C and 8°C ($p < 0.05$) (Table 6). For *P. antarctica*, the Chl *a*

285   per cell values at 100 ppm, 205 ppm, and 755 ppm CO_2 at 8°C were significantly lower relative

286   to 2°C ($p < 0.05$) (Table 6). Temperature increase and CO_2 concentration increase interactively

287   increased the C and N quotas of *P. antarctica* ($p < 0.05$) (Table 6).

288   **4 Discussion**

289   As has been documented in previous work, the diatom *P. subcurvata* and the

290   prymnesiophyte *P. antarctica* responded differently to warming (Xu et al., 2014; Zhu et al.

291   2016). In the Southern Ocean as elsewhere, temperature determines both phytoplankton

292   maximum growth rates (Bissinger et al., 2008) and the upper limit of growth (Smith, 1990) in a

293   species-specific manner. Thermal functional responses curves of phytoplankton typically

294   increase in a normally distributed pattern, with growth rates increasing up to the optimum

295   temperature range, and then declining when temperature reaches inhibitory levels (Boyd et al.,

296   2013; Fu et al., 2014; Xu et al., 2014). Specific growth rates of *P. subcurvata* reached optimal

297   levels at 8°C, while those of *P. antarctica* saturated at 2°C. Zhu et al. (2016) found that 4°C

298   warming significantly promoted the growth rates of *P. subcurvata* but not *P. antarctica*. Xu et al.

299   (2014) found that the growth rates of another strain of *P. antarctica* (CCMP3314) decreased in a

300   multi-variable "year 2100 cluster" condition (6°C, 81 Pa CO_2, 150 µmol photons m^{-2} s^{-1})

301   relative to the "current condition" (2°C, 39 Pa CO_2, and 50 µmol photons m^{-2} s^{-1}) and the "year

302   2060 condition" (4°C, 61 Pa CO_2, and 100 µmol photons m^{-2} s^{-1}). In our study, the Q10 value of

303   *P. subcurvata* from 0°C to 4°C was 3.11, nearly 50% higher than the Q10 value of *P. antarctica*

304   across the same temperature range (2.17), and similar to the Q10 values observed for different

305   strains of these two species in Zhu et al. (2016). Our results showed that the maximal thermal

306   limit of *P. antarctica* was reached at 10°C, as was also observed by Buma et al. (1991), while *P.*

307   *subcurvata* did not cease to grow until 14°C. Clearly, *P. subcurvata* has a superior tolerance to

308   higher temperature compared to *P. antarctica*.

309   The competition experiment between *P. subcurvata* and *P. antarctica* at 0°C and 6°C

310   confirmed that the diatom had an additional competitive advantage over *P. antarctica* at the

311   higher temperature. Xu el al. (2014) observed that the diatom *Fragilariopsis cylindrus* also

312   outcompeted *P. antarctica* under "year 2060 conditions" (4°C, 61 Pa CO_2, and 100 µmol

313   photons m^{-2} s^{-1}). These competition experiments support the results of a Ross Sea field survey

314   which suggested that water temperature structured the phytoplankton assemblage (Liu and

315   Smith, 2012), and may shed light on why *P. antarctica* is often dominant in cooler waters in the

316   springtime, while diatoms often dominate in summer (DiTullio and Smith, 1996; Arrigo et al.,

317   1999; DiTullio et al., 2000; Liu and Smith, 2012).

318   Besides temperature, mixed layer depth and light intensity also likely play a role in the

319   competition between diatoms and *P. antarctica* (Arrigo et al., 1999; Arrigo et al., 2010). Arrigo

320   et al. (1999) observed that *P. antarctica* dominated the southern Ross Sea region with deeper

321   mixed layers, while diatom dominated the regions with shallower mixed layer depths. To some

322   extent temperature and irradiance can often be considered co-variables, as shallow surface

323   stratification promotes both solar heating and high irradiance, while deep mixing lowers both

324   light and temperatures. Thus, rather than being segregated by either light or by temperature, it is

325   worth considering whether these two phytoplankton groups are each best adapted to a different

326   environmental matrix of both variables. This concept of different light/temperature niches for

327   Ross Sea diatoms and *P. antarctica* is worthy of further investigation.

328   Temperature change affected the C: P, N: P and C: Si ratios of *P. subcurvata*, due to the

329   combined effects of the different responses of cellular C, P, and Si quotas. The C: P and N:P

330   ratios of *P. subcurvata* increased at the two highest temperatures tested. This might be due to an

331   increase in protein translation efficiency and a corresponding decrease in phosphate-rich

332   ribosomes with warming, which can result in a decreased cellular P requirement per unit of

333   carbon in marine phytoplankton (Toseland et al., 2013). Similarly lowered P quotas at higher

334   temperatures have been documented in other studies as well (Xu et al., 2014; Boyd et al., 2015;

335   Hutchins and Boyd, 2016). This result suggests that the amount of carbon exported per unit

336   phosphorus by *P. subcurvata* (and perhaps other diatoms) in the Southern Ocean may increase as

337   temperature increases in the future (Toseland et al., 2013).

338   In contrast, the decreasing trend of C: Si ratios in *P. subcurvata* appears to be largely due

339   to higher cellular Si quotas at temperatures at and above 4°C. Although the physiological

340   reason(s) for increased silicification with warming are currently not understood, this trend also

341   may have significant biogeochemical consequences. These results suggest that Si export by

342   diatoms in the Southern Ocean could be enhanced under future global warming.

343   Previous studies have shown that nutrient drawdown by diatoms and *P. antarctica* are

344   different, due to differing elemental ratios of these two groups (Arrigo et al., 1999; Xu et al.,

345   2014). Our results generally corresponded to this trend, as the N: P ratios of *P. antarctica* were

346   higher than *P. subcurvata* at 2°C, 6°C and 8°C and C: P ratios of *P. antarctica* were higher than

347   *P. subcurvata* at 6°C and 8°C ($p < 0.05$) (Fig. 2). Although elemental ratios of the

348   prymnesiophyte were largely unaffected by temperature. phytoplankton relative abundance shifts

349   caused by warming (such as those observed in our competition experiment) will likely change

350   nutrient export ratios. Thus, N and C export per unit P may decrease with a phytoplankton

351   community shift from *P. antarctica* dominance to diatom dominance (Arrigo et al., 1999; Xu et

352   al., 2014).

353   Our results showed that the growth rates of both *P. subcurvata* and *P. antarctica*

354   exhibited moderate limitation by CO_2 levels lower than ~425 ppm at both 2°C and 8°C; this

355   observation is significant, since pCO_2 during the intense Ross Sea summertime phytoplankton

356   bloom can sometimes drop to very low levels (Tagliabue and Arrigo, 2016). However, at CO_2

357   concentrations beyond current atmospheric levels of ~400 ppm, growth rates of *P. subcurvata* or

358   *P. antarctica* were CO_2-saturated. Although a general model prediction suggests that an

359   atmospheric CO_2 increase from current levels to 700 ppm could increase the growth of marine

360   phytoplankton by 40% (Schippers et al., 2004), our results instead correspond to several other

361   studies which showed negligible effects of elevated CO_2 on different groups of phytoplankton,

362   including *P. subcurvata* and *P. antarctica* (Goldman, 1999; Fu et al., 2007, Trimborn et al.,

363   2013). The minimal effects of CO_2 levels higher than 400 ppm on these phytoplankton has been

364   suggested to be due to efficient carbon concentrating mechanisms (CCMs) (Burkhardt et al.,

365   2001; Fu et al., 2007; Tortell et al., 2008; Trimborn et al., 2013), although clearly for our two

366   species their CCM activity was not sufficient to completely compensate for carbon limitation at

367   low pCO_2 levels. Our results also showed that very high CO_2 (1730 ppm) significantly reduced

368   the growth rate of *P. antarctica* relative to 425 ppm and 755 ppm at 2°C; negative effects of high

369   CO_2 on an Antarctic microbial community were also observed by Davidson et al. (2016). This

370   inhibitory effect might be due to the significantly lower pH at 1730 ppm (~7.4), which could

371   entail expenditures of additional energy to maintain pH homeostasis within cells.

372   Warming from 2°C to 8°C had a significant interactive effect with CO_2 concentration in

373   *P. subcurvata*, as maximum growth rates were higher and the half saturation constant ($K_{1/2}$) for

374   growth was much lower at the warmer temperature. In contrast, warming decreased the maximal

375   growth rates of *P. antarctica* over the range of CO_2 concentrations tested, and failed to change its

376    $K_{1/2}$ for growth. The decreased CO_2 $K_{1/2}$ of *P. subcurvata* at high temperature might confer a

377   future additional competitive advantage over *P. antarctica* in the late growing season when pCO_2

378   can be low (Tagliabue and Arrigo, 2016) and temperatures higher, although temperatures are

379   generally never as high as 8°C in the current Ross Sea (Liu and Smith, 2012). The CO_2 $K_{1/2}$ of *P.*

380   *antarctica* at 2°C was however significantly lower than that of *P. subcurvata* at this temperature,

381   which may be advantageous to the prymnesiophyte when water temperatures are low in the

382   spring.

383   The effects of pCO_2 variation on the elemental ratios of *P. subcurvata* and *P. antarctica*

384   were minimal relative to those of temperature increase. Previous research on the effects of CO_2

385   on the elemental ratios of phytoplankton has shown that the elemental composition of

386   phytoplankton may change with CO_2 availability (Burkhardt et al., 1999; Fu et al., 2007, 2008;

387   Tew et al., 2014; reviewed in Hutchins et al., 2009). Hoogstraten et al. (2012) found that CO_2

388   concentration change didn't change the cellular POC, PON, C: N ratios, or POC to Chl *a* ratios

389   of the temperate species *Phaeocystis globosa*. In contrast, Reinfelder (2014) observed that the N

390   and P quotas of several diatoms decreased with increasing CO_2 and led to increased C: N, N: P,

391   and C: P ratios. King et al. (2015) found that high CO_2 could increase, decrease or not affect the

392   C: P and N: P ratios of several different phytoplankton species. Our results resemble those of

393   studies with other phytoplankton that found that the effects of CO_2 concentration can be

394   negligible on C: N, N: P, or C: P ratios (Fu et al., 2007; Hutchins et al., 2009; Hoogstraten et al.,

395   2012; King et al., 2015).

396   In contrast to C:N:P ratios, we observed that the C: Si ratios of *P. subcurvata* were

397   significantly higher at 1730 ppm compared to almost all of the lower CO_2 levels. This increase in

398   C: Si ratios was due to a decrease in cellular Si quotas at 1730 ppm CO_2. Milligan et al. (2004)

399   observed that the silica dissolution rates of a temperate diatom increased significantly in high

400   CO_2 relative to in low CO_2 cultures. Tatters et al. (2012) found a similar trend in the temperate

401   toxic diatom *Pseudo-nitzschia fraudulenta*, in which cellular C: Si ratios were higher at 765 ppm

402   than at 200 ppm CO_2. This suggests that future increases in diatom silicification at elevated

403   pCO_2 could partially or wholly offset the decreased silicification observed at warmer

404   temperatures (above); to fully predict net trends, further interactive experiments focusing on

405   silicification as a function across a range of both temperature and pCO_2 are needed.

406   In conclusion, our results indicate that *P. subcurvata* from the Ross Sea are better adapted

407   to higher temperature than is *P. antarctica*, suggesting that the relative dominance of *P.*

408   *antarctica* in this region may wane in under future global warming scenarios. Such an ecological

409   shift may significantly change the biogeochemical cycles of carbon, nitrogen, phosphorus,

410   silicon, and sulfur. This conclusion must be qualified as it was obtained using Fe-replete culture

411   conditions; which often prevail early in the growing season in McMurdo Sound. However, Fe

412   limitation generally prevails later in the season here, and elsewhere in the offshore Ross Sea.

413   Irradiance is another key environmental factor to consider in both the present and future in this

414   region. Thus, in addition to warming and CO_2 increases, the interactive effects of light and Fe

415   with these two factors should also be considered (Xu et al., 2014; Boyd et al., 2015). Considering

416   the differences between the responses of the diatom and *P. antarctica* to warming and ocean

417   acidification seen here, as well to warming and Fe in previous work (Zhu et al., 2016), models

418   attempting to predict future changes in community structure and primary production in Southern

419   Ocean coastal polynyas may need to realistically incorporate a complex network of interacting

420   global change variables.

421

422   **Author contribution**

423   Z. Zhu, F. X. Fu, D. A. Hutchins designed the experiments, Z. Zhu, P. Qu, and J. Gale carried

424   them out, and Z. Zhu and D. A. Hutchins wrote the manuscripts.

425   **Competing interests**

426   The authors declare that they have no conflict of interest.

427   **Acknowledgments**

430   **References**

Biogeosciences
Open Access
EGU
Discussions

431 Arrigo, K. R., Robinson, D. H., Worthen, D. L., Dunbar, R. B., DiTullio, G. R., VanWoert, M.,

432 and Lizotte, M. P.: Phytoplankton community structure and the drawdown of nutrients and CO_2

433 in the Southern Ocean, Science, 283, 365-367, 1999.

434 Arrigo K. R., DiTullio G. R., Dunbar R. B., Robinson D. H., Van Woert M., Worthen D. L.,

435 Lizotte M. P.: Phytoplankton taxonomic variability in nutrient utilization and primary production

436 in the Ross Sea, J. Geophys Res: Oceans, 105, 8827-8846, 2000.

437 Arrigo, K. R., van Dijken, G. L., and Bushinsky, S.: Primary production in the Southern Ocean,

438 1997–2006, J. Geophys Res, 113, C08004, doi:10.1029/2007JC004551, 2008.

439 Arrigo, K. R., Mills, M. M., Kropuenske, L. R., van Dijken, G. L., Alderkamp, A. C., and

440 Robinson, D. H.: Photophysiology in two major Southern Ocean phytoplankton taxa:

441 photosynthesis and growth of *Phaeocystis antarctica* and *Fragilariopsis cylindrus* under

442 different irradiance levels, Integrative and Comparative Biology, 50(6), 950-966, 2010.

443 Bertrand, E.M., McCrow, J.P., Zheng, H., Moustafa, A., McQuaid, J., Delmont, T., Post, A.,

444 Sipler, R., Spackeen, J., Xu, K., Bronk, D., Hutchins, D.A., and Allen, A.E.: Phytoplankton-

445 bacterial interactions mediate micronutrient colimitation in the Southern Ocean, P. Natl. Acad.

446 Sci. USA, 112. doi:10.1073/pnas.1501615112, 2015.

447 Bissinger, J. E., Montagnes, D. J., Sharples, J., and Atkinson, D.: Predicting marine

448 phytoplankton maximum growth rates from temperature: Improving on the Eppley curve using

449 quantile regression, Limnol. Oceanogr., 53, 487, 2008.

450 Boyd, P. W., Rynearson, T. A., Armstrong, E. A., Fu, F., Hayashi, K., Hu, Z., Hutchins, D.A.,

451 Kudela, R.M., Litchman, E., Mulholland, M.R. and Passow, U.: Marine phytoplankton

452 temperature versus growth responses from polar to tropical waters–outcome of a scientific

453 community-wide study, PLoS One, 8, available at:

454 http://dx.doi.org/10.1371/journal.pone.0063091, 2013.

455 Boyd, P. W., Dillingham, P. W., McGraw, C. M., Armstrong, E. A., Cornwall, C. E., Feng, Y.

456 Y., Hurd, C.L., Gault-Ringold, M., Roleda, M.Y., Timmins-Schiffman, E. and Nunn, B. L.:

Biogeosciences

Discussions

Open Access

EGU

457   Physiological responses of a Southern Ocean diatom to complex future ocean conditions, Nature

458   Climate Change, 6, 207-213, 2015.

459   Buma, A. G. J., Bano, N., Veldhuis, M. J. W., and Kraay, G. W.: Comparison of the

460   pigmentation of two strains of the prymnesiophyte *Phaeocystis* sp., Neth. J. Sea Res., 27(2), 173-

461   182, 1991.

462   Burkhardt, S., Zondervan, I., and Riebesell, U.: Effect of CO_2 concentration on C: N: P ratio in

463   marine phytoplankton: A species comparison, Limnol. Oceanogr., 44, 683-690, 1999.

464   Burkhardt, S., Amoroso, G., Riebesell, U., and Sültemeyer, D.: CO_2 and HCO_3^{-1} uptake in

465   marine diatoms acclimated to different CO_2 concentrations, Limnol. Oceanogr., 46, 1378-1391,

466   2001.

467   Caron, D. A., Dennett, M. R., Lonsdale, D. J., Moran, D. M., and Shalapyonok, L.:

468   Microzooplankton herbivory in the Ross sea, Antarctica, Deep-Sea Res. Pt. II, 47(15), 3249-

469   3272, 2000.

470   Chaui-Berlinck, J. G., Monteiro, L. H. A., Navas, C. A., and Bicudo, J. E. P.: Temperature

471   effects on energy metabolism: a dynamic system analysis, P. Roy. Soc. Lond. B Bio., 269, 15-19,

472   2002.

473   Davidson, A. T., McKinlay, J., Westwood, K., Thompson, P. G., van den Enden, R., de Salas,

474   M., Wright, S., Johnson, R., and Berry, K.: Enhanced CO_2 concentrations change the structure of

475   Antarctic marine microbial communities, Mar. Ecol-Prog. Ser., 552, 92-113, 2016.

476   DiTullio, G. R., and Smith, W. O.: Spatial patterns in phytoplankton biomass and pigment

477   distributions in the Ross Sea. J. Geophys Res: Oceans, 101, 18467-18477, 1996.

478   DiTullio, G. R., Grebmeier, J. M., Arrigo, K. R., Lizotte, M. P., Robinson, D. H., Leventer, A.,

479   Barry, J.P., VanWoert, M.L. and Dunbar, R. B.: Rapid and early export of *Phaeocystis*

480   *antarctica* blooms in the Ross Sea, Antarctica, Nature, 404, 595-598, 2000.

481   El-Sabaawi, R., and Harrison, P. J.: Interactive effects of irradiance and temperature on the

482   photosynthetic physiology of the pennate diatom *Pseudo-nitzschia Granii* (Bacillariophyceae)

483   from the northeast Subarctic Pacific, J. Phycol., 42, 778-785, 2006.

Biogeosciences Open Access
Discussions
EGU

484   Fabry, V. J. (2008). Marine calcifiers in a high-CO_2 ocean. *Science*, 320(5879), 1020-1022.

485   Fu, F. X., Warner, M. E., Zhang, Y., Feng, Y., and Hutchins, D. A.: Effects of increased

486   temperature and CO_2 on photosynthesis, growth, and elemental ratios in marine *Synechococcus*

487   and *Prochlorococcus* (cyanobacteria), J. Phycol., 43, 485-496, 2007.

488   Fu, F. X., Zhang, Y., Warner, M. E., Feng, Y., Sun, J., and Hutchins, D. A.: A comparison of

489   future increased CO_2 and temperature effects on sympatric *Heterosigma akashiwo* and

490   *Prorocentrum minimum*, Harmful Algae, 7, 76-90, 2008.

491   Fu, F. X., Yu, E., Garcia, N. S., Gale, J., Luo, Y., Webb, E. A., and Hutchins, D. A.: Differing

492   responses of marine N_2 fixers to warming and consequences for future diazotroph community

493   structure, Aquat. Microb. Ecol., 72, 33-46, 2014.

494   Gille, S. T.: Warming of the Southern Ocean since the 1950s, Science, 295, 1275-1277, 2002.

495   Goldman, J. C.: Inorganic carbon availability and the growth of large marine diatoms, *Mar.*

496   *Ecol-Prog. Ser.*, 180, 81-91, 1999.

497   Hoogstraten, A., Peters, M., Timmermans, K. R., and De Baar, H. J. W.: Combined effects of

498   inorganic carbon and light on *Phaeocystis globosa* Scherffel

499   (Prymnesiophyceae), Biogeosciences, 9, 1885-1896, 2012.

500   Hutchins, D.A., Mulholland, M.R. and Fu, F. X.: Nutrient cycles and marine microbes in a CO_2-

501   enriched ocean, Oceanography, 22: 128-145, 2009.

502   Hutchins, D.A. and Boyd, P.W.: Marine phytoplankton and the changing ocean iron cycle,

503   Nature Climate Change, 6: 1071-1079, 2016.

504   IPCC, 2014: Climate Change 2014: Impacts, Adaptation, and Vulnerability. Part A: Global and

505   Sectoral Aspects. Contribution of Working Group II to the Fifth Assessment Report of the

506   Intergovernmental Panel on Climate Change.

507   King, A. L., Sanudo-Wilhelmy, S. A., Leblanc, K., Hutchins, D. A., and Fu, F. X.: CO_2 and

508   vitamin B12 interactions determine bioactive trace metal requirements of a subarctic Pacific

509   diatom, The ISME J., 5, 1388-1396, 2011.

Biogeosciences Open Access
EGU
Discussions

510 King, A. L., Jenkins, B. D., Wallace, J. R., Liu, Y., Wikfors, G. H., Milke, L. M., and Meseck, S.

511 L.: Effects of CO_2 on growth rate, C: N: P, and fatty acid composition of seven marine

512 phytoplankton species, Mar. Ecol-Prog. Ser., 537, 59-69, 2015.

513 Knox, G. A.: The Biology of the Southern Ocean, Cambridge University Press, New York, USA,

514 1994.

515 Liu, X., and Smith, W. O.: Physiochemical controls on phytoplankton distributions in the Ross

516 Sea, Antarctica, J. Marine Syst., 94, 135-144, 2012.

517 Milligan, A. J., Varela, D. E., Brzezinski, M. A., and Morel, F. M.: Dynamics of silicon

518 metabolism and silicon isotopic discrimination in a marine diatom as a function of

519 pCO_2, Limnol. Oceanogr, 49, 322-329, 2004.

520 Orr, J. C., Fabry, V. J., Aumont, O., Bopp, L., Doney, S. C., Feely, R. A., Gnanadesikan, A.,

521 Gruber, N., Ishida, A., Joos, F. and Key, R. M.: Anthropogenic ocean acidification over the

522 twenty-first century and its impact on calcifying organisms, Nature, 437, 681-686, 2005.

523 Paasche, E.: Silicon and the ecology of marine plankton diatoms. II. Silicate-uptake kinetics in

524 five diatom species, Mar. Biol., 19, 262-269, 1973.

525 Reinfelder, J. R.: Carbon dioxide regulation of nitrogen and phosphorus in four species of marine

526 phytoplankton, Mar. Ecol-Prog. Ser., 466, 57-67, 2012.

527 Pierrot, D., Lewis, E., and Wallace, D. W. R.: MS Excel program developed for CO_2 system

528 calculations. ORNL/CDIAC-105a. Carbon Dioxide Information Analysis Center, Oak Ridge

529 National Laboratory, US Department of Energy, Oak Ridge, Tennessee, 2006.

530 Rose, J. M., Feng, Y., DiTullio, G. R., Dunbar, R. B., Hare, C. E., Lee, P. A., Lohan, M.C.,

531 Long, M.C., Smith, W.O., Sohst, B.M., and Tozzi, S.: Synergistic effects of iron and temperature

532 on Antarctic phytoplankton and microzooplankton assemblages, Biogeosciences, 6, 3131-3147,

533 2009.

534 Sarmiento, J. L., Hughes, T. M., Stouffer, R. J., and Manabe, S.: Simulated response of the ocean

535 carbon cycle to anthropogenic climate warming, Nature, 393, 245-249, 1998.

Biogeosciences
Open Access
EGU
Discussions

536   Schippers, P., Lürling, M., and Scheffer, M.: Increase of atmospheric CO_2 promotes

537   phytoplankton productivity, Ecol. Lett, 7, 446-451, 2004.

538   Schoemann V., Becquevort S., Stefels J., Rousseau V., Lancelot C.: *Phaeocystis* blooms in the

539   global ocean and their controlling mechanisms: a review, J. Sea Res., 53, 43-66, 2005.

540   Smith, W. O.: Polar Oceanography, Chemistry, Biology and Geology, Academic Press,

541   Massachusetts, USA, 1990.

542   Smith, W. O., Marra, J., Hiscock, M. R., and Barber, R. T.: The seasonal cycle of phytoplankton

543   biomass and primary productivity in the Ross Sea, Antarctica, Deep-Sea Res. Pt. II, 47, 3119-

544   3140, 2000.

545   Tagliabue, A., and Arrigo, K.R.: Decadal trends in air-sea CO_2 exchange in the Ross Sea

546   (Antarctica), Geophys. Res. Lett., 43: 5271-5278, 2016.

547   Tatters, A.O., Fu, F.X. and Hutchins, D.A.: High CO_2 and silicate limitation synergistically

548   increase the toxicity of *Pseudo-nitzshia fraudulenta*, *PLoS ONE*, 7, available at:

549   http://dx.doi.org/10.1371/journal.pone.0032116, 2012.

550   Tew, K. S., Kao, Y. C., Ko, F. C., Kuo, J., Meng, P. J., Liu, P. J., and Glover, D. C.: Effects of

551   elevated CO_2 and temperature on the growth, elemental composition, and cell size of two marine

552   diatoms: potential implications of global climate change, Hydrobiologia, 741, 79-87, 2014.

553   Thomas, M. K., Kremer, C. T., Klausmeier, C. A., and Litchman, E.: A global pattern of thermal

554   adaptation in marine phytoplankton, Science, 338, 1085-1088, 2012.

555   Tortell, P. D., Payne, C., Gueguen, C., Li, Y., Strzepek, R. F., Boyd, P. W., and Rost, B., Uptake

556   and assimilation of inorganic carbon by Southern Ocean phytoplankton. Limnol. Oceanogr., 53,

557   1266-1278, 2008.

558   Toseland, A. D. S. J., Daines, S. J., Clark, J. R., Kirkham, A., Strauss, J., Uhlig, C., Lenton,

559   T.M., Valentin, K., Pearson, G.A., Moulton, V. and Mock, T. (2013). The impact of temperature

560   on marine phytoplankton resource allocation and metabolism. *Nature Climate Change*, 3(11),

561   979-984.

562   Treguer, P., Nelson, D. M., Van Bennekom, A. J., and DeMaster, D. J.: The silica balance in the

563   world ocean: a reestimate, Science, *268*, 375, 1995.

564   Trimborn, S., Brenneis, T., Sweet, E., and Rost, B.: Sensitivity of Antarctic phytoplankton

565   species to ocean acidification: Growth, carbon acquisition, and species interaction, Limnol.

566   Oceanogr., 58, 997-1007, 2013.

567   Wang, Y., Smith, W. O., Wang, X., and Li, S.: Subtle biological responses to increased CO_2

568   concentrations by *Phaeocystis globosa* Scherffel, a harmful algal bloom species, Geophys. Res.

569   Lett., 37, L09604, doi:10.1029/2010GL042666, 2010.

570   Xu, K., Fu, F. X., and Hutchins, D. A.: Comparative responses of two dominant Antarctic

571   phytoplankton taxa to interactions between ocean acidification, warming, irradiance, and iron

572   availability, Limnol. Oceanogr., *59*, 1919-1931, 2014.

573   Zhu, Z., Xu, K., Fu, F., Spackeen, J. L., Bronk, D. A., and Hutchins, D. A.: A comparative study

574   of iron and temperature interactive effects on diatoms and *Phaeocystis antarctica* from the Ross

575   Sea, Antarctica, Mar. Ecol-Prog. Ser., 550, 39-51, 2016.

576

Biogeosciences
Discussions

Open Access

EGU

577   Table 1. The measured pH and dissolved inorganic carbon (DIC), and calculated pCO_2 of *P. subcurvata*

578   and *P. antarctica* at 2°C and 8°C in each treatment. Values represent the means and errors are the

579   standard deviations of triplicate bottles.

580

	P. subcurvata		*P. antarctica*	
	2°C	8°C	2°C	8°C
pH				
	8.36±0.04	8.51±0.04	8.40±0.03	8.45±0.03
	8.25±0.04	8.36±0.01	8.22±0.04	8.29±0.01
	8.07±0.01	8.17±0.01	8.09±0.02	8.14±0.00
	7.86±0.02	7.99±0.01	7.85±0.01	7.94±0.00
	7.68±0.01	7.79±0.02	7.65±0.01	7.75±0.00
	7.35±0.01	7.46±0.02	7.34±0.01	7.45±0.00
DIC (μmol/kg)				
	1890.1±26.6	1846.5±15.8	1847.1±30.0	1831.1±22.7
	2049.1±10.8	1985.7±2.1	2033.9±15.0	2014.2±19.9
	2131.3±9.4	2067.5±4.7	2136.6±5.6	2085.3±15.3
	2190.4±2.8	2156.1±13.9	2168.1±12.4	2167.4±21.5
	2260.0±22.2	2234.8±10.3	2252.1±11.5	2238.7±12.0
	2340.1±19.4	2334.5±18.8	2338.2±12.1	2323.7±11.5
pCO_2 (ppm)				
	109.1±9.3	94.4±10.1	96.6±9.5	108.8±8.8
	158.6±15.5	150.3±3.6	171.2±14.4	183.6±4.2
	263.1±5.9	254.2±9.9	246.4±9.9	280.3±0.6
	450.2±17.3	414.9±12.0	462.2±12.1	480.9±4.7
	740.9±10.6	708.8±23.5	786.9±10.3	784.1±4.8
	1751.2±35.9	1675.3±49.4	1769.9±59.5	1720.3±18.3

581
582
583

584   Table 2. Statistical comparison of the results for each of the three thermal traits: Optimum temperature

585   (ºC), Maximum growth rate (d^{-1}) and temperature niche width (W)* of *P. subcurvata* and *P. antarctica.*

586

Species	Optimum temperature (ºC)	Maximum growth rates (d^{-1})	W upper CI	W lower CI	Q_{10}
P. subcurvata	7.36	0.86	12.19	< -2.0	3.17
P. antarctica	4.85	0.66	9.52	< -2.0	2.11

587
588   *   The statistical results for the lower bound of temperate niche width in both species were lower
589   than -2.0ºC, the freezing point of seawater
590

591 Table 3. The effects of temperature on the C quota (pmol cell^{-1}), N quota (pmol cell^{-1}), P quota (pmol

592 cell^{-1}), Si quota (pmol cell^{-1}), and chl *a* per cell (pg cell^{-1}) of *P. subcurvata* and *P. antarctica*. Values

593 represent the means and errors are the standard deviations of triplicate bottles.

594

	P. subcurvata	*P. antarctica*
C quota		
0°C	1.91±0.14	2.64±0.34
2°C	2.11±0.19	2.49±0.41
4°C	2.15±0.12	2.50±0.23
6°C	2.07±0.13	2.26±0.18
8°C	2.33±0.14	2.17±0.22
10°C	2.17±0.13	
N quota		
0°C	0.27±0.03	0.39±0.03
2°C	0.29±0.03	0.36±0.02
4°C	0.33±0.02	0.40±0.01
6°C	0.31±0.01	0.35±0.02
8°C	0.36±0.05	0.34±0.03
10°C	0.33±0.04	
P quota		
0°C	0.02±0.00	0.03±0.00
2°C	0.02±0.00	0.02±0.00
4°C	0.03±0.00	0.03±0.01
6°C	0.03±0.00	0.02±0.00
8°C	0.03±0.00	0.02±0.00
10°C	0.02±0.00	
Si quota		
0°C	0.23±0.02	
2°C	0.23±0.06	
4°C	0.30±0.01	
6°C	0.30±0.03	
8°C	0.34±0.01	
10°C	0.28±0.04	
Chl a per cell (pg/cell)		
0°C	0.48±0.01	0.23±0.03
2°C	0.57±0.07	0.22±0.02
4°C	0.64±0.01	0.20±0.01
6°C	0.68±0.05	0.21±0.00
8°C	0.58±0.03	0.17±0.02
10°C	0.46±0.03	

595
596
597

598   Table 4. Comparison of the curve fitting results for maximum growth rate (d^{-1}) and half saturation

599   constants (K_m), calculated from the CO_2 functional response curves of *P. subcurvata* and *P. antarctica* at

600   2°C and 8°C. Values represent the means and errors are the standard errors from fitting.

601   .

Species	Maximum growth rates (d^{-1})	K_m
P. subcurvata		
2°C	0.60±0.18	66.4±10.39
8°C	0.88±0.02	9.8±5.34
P. antarctica		
2°C	0.61±0.02	26.4±8.23
8°C	0.41±0.02	22.1±11.15

602

603   Table 5 The effects of CO_2 on the C: N, N: P, C: P, C: Si, and C: Chl *a* ratios of *P. subcurvata* and *P.*

604   *antarctica* at 2°C and 8°C. Values represent the means and errors are the standard deviations of triplicate

605   bottles.

	P. subcurvata		*P. antarctica*	
	2°C	8°C	2°C	8°C
C: N				
100 ppm	6.6±0.26	7.1±0.68	7.22±0.50	6.95±0.35
205 ppm	6.7±0.24	7.5±0.32	7.74±0.21	6.56±1.15
260 ppm	6.7±0.32	7.3±0.18	8.07±0.52	6.99±0.27
425 ppm	6.7±0.05	6.6±0.05	7.21±0.81	6.19±0.13
755 ppm	6.8±0.20	7.1±0.68	7.98±0.44	6.79±0.22
1730 ppm	7.1±0.82	7.4±1.07	8.15±0.48	7.05±0.91
N: P				
100 ppm	10.4±0.85	14.5±2.28	16.4±1.24	13.9±0.20
205 ppm	10.8±1.01	13.3±0.42	16.6±1.12	15.7±2.77
260 ppm	10.3±1.28	14.0±0.56	14.3±1.24	14.5±2.38
425 ppm	11.3±0.84	16.5±0.28	17.1±1.83	17.2±1.98
755 ppm	9.9±0.28	14.3±1.34	14.2±2.60	11.6±4.11
1730 ppm	10.4±1.02	15.5±1.84	15.5±0.56	15.1±1.85
C: P				
100 ppm	68.6±3.10	101.0±6.43	117.7±4.08	96.7±4.86
205 ppm	72.7±4.82	99.3±7.05	128.2±5.98	101.0±1.91
260 ppm	69.1±7.68	103.0±4.88	115.5±7.25	101.0±13.04
425 ppm	76.3±5.19	109.0±2.20	122.3±4.85	106.0±11.14
755 ppm	67.2±1.38	101.0±5.80	113.5±22.50	78.6±27.09
1730 ppm	73.4±1.22	114.0±5.99	126.2±12.10	105.0±6.26
C: Si				
100 ppm	7.8±0.80	5.6±0.32		
205 ppm	7.4±0.30	5.6±0.24		
260 ppm	7.3±0.23	6.1±0.38		
425 ppm	7.5±0.23	6.1±0.06		
755 ppm	7.4±0.66	6.3±0.36		
1730 ppm	8.0±0.88	7.1±0.47		
C: Chl *a* (μg/μg)				
100 ppm	43.6±1.14	70.7±5.01	160.4±6.68	197.4±29.35
205 ppm	45.2±2.91	67.3±4.42	157.5±4.95	194.0±17.14
260 ppm	41.6±3.31	60.1±9.45	138.3±15.19	169.8±9.20
425 ppm	37.2±2.58	72.5±2.35	180.2±20.10	232.4±20.47
755 ppm	42.2±3.62	68.7±6.29	167.5±5.06	282.5±15.30
1730 ppm	46.3±2.23	85.3±15.70	276.5±36.57	460.3±15.21

606
607
608
609
610
611
612

613   Table 6 The effects of CO_2 on the C quota (pmol cell^{-1}), N quota (pmol cell^{-1}), P quota (pmol cell^{-1}), Si

614   quota (pmol cell^{-1}), and chl *a* per cell (pg cell^{-1}) of *P. subcurvata* and *P. antarctica* at 2°C and 8°C.

615   Values represent the means and errors are the standard deviations of triplicate bottles.

	P. subcurvata		*P. antarctica*	
	2°C	8°C	2°C	8°C
C quota				
100 ppm	2.0±0.15	2.64±0.06	2.57±0.03	2.15±0.22
205 ppm	2.1±0.12	2.67±0.31	2.72±0.28	2.35±0.19
260 ppm	1.9±0.04	2.28±0.18	2.51±0.36	2.21±0.04
425 ppm	1.8±0.04	2.43±0.15	2.31±0.05	2.28±0.46
755 ppm	2.1±0.09	2.26±0.05	2.47±0.17	2.81±0.15
1730 ppm	2.1±0.30	2.47±0.18	2.43±0.10	2.96±0.30
N quota				
100 ppm	0.30±0.03	0.38±0.04	0.36±0.03	0.31±0.03
205 ppm	0.30±0.03	0.36±0.03	0.35±0.03	0.36±0.06
260 ppm	0.29±0.01	0.31±0.02	0.31±0.06	0.32±0.02
425 ppm	0.27±0.01	0.37±0.06	0.32±0.03	0.37±0.05
755 ppm	0.30±0.02	0.32±0.03	0.31±0.03	0.41±0.01
1730 ppm	0.29±0.05	0.34±0.06	0.30±0.03	0.43±0.10
P quota				
100 ppm	0.03±0.00	0.03±0.00	0.02±0.00	0.02±0.00
205 ppm	0.03±0.00	0.03±0.00	0.02±0.00	0.02±0.00
260 ppm	0.03±0.00	0.02±0.00	0.02±0.00	0.02±0.00
425 ppm	0.02±0.00	0.02±0.00	0.02±0.00	0.02±0.01
755 ppm	0.03±0.00	0.02±0.00	0.02±0.00	0.04±0.02
1730 ppm	0.03±0.00	0.02±0.00	0.02±0.00	0.03±0.00
Si quota				
100 ppm	0.26±0.02	0.47±0.04		
205 ppm	0.28±0.02	0.48±0.07		
260 ppm	0.27±0.01	0.37±0.03		
425 ppm	0.25±0.01	0.40±0.04		
755 ppm	0.28±0.03	0.36±0.03		
1730 ppm	0.26±0.01	0.35±0.05		
Chl a per cell (pg/cell)				
100 ppm	0.54±0.05	0.45±0.04	0.19±0.01	0.13±0.02
205 ppm	0.54±0.04	0.48±0.05	0.21±0.02	0.15±0.02
260 ppm	0.56±0.03	0.46±0.04	0.22±0.04	0.16±0.01
425 ppm	0.60±0.04	0.40±0.04	0.16±0.02	0.12±0.01
755 ppm	0.59±0.06	0.40±0.03	0.18±0.01	0.12±0.00
1730 ppm	0.53±0.06	0.35±0.05	0.11±0.02	0.08±0.01

616
617
618

Biogeosciences
Discussions

Open Access

EGU

619
620 **Figure legends**

621 Fig. 1. Thermal functional response curves showing specific growth rates (and fitted curves) of

622 *Pseudo-nitzschia subcurvata* and *Phaeocystis antarctica* across a range of temperatures from 0^oC

623 to 14^oC. Values represent the means and error bars represents the standard deviations of triplicate

624 samples.

625

626 Fig. 2. The C: N ratios (A), N: P ratios (B), and C: P ratios (C) of *Pseudo-nitzschia subcurvata*

627 and *Phaeocystis antarctica* and (D) the C: Si ratios of *Pseudo-nitzschia subcurvata* from the

628 thermal response curves shown in Fig. 1 for a range of temperatures from 0^oC to 10^oC. Values

629 represent the means and error bars represents the standard deviations of triplicate samples.

630

631 Fig. 3. The C: Chl *a* ratios of *Pseudo-nitzschia subcurvata* and *Phaeocystis antarctica* from the

632 thermal response curves shown in Fig. 1 for a range of temperatures from 0^oC to 10^oC. Values

633 represent the means and error bars represents the standard deviations of triplicate samples.

634 .

635 Fig. 4. The relative abundance of *Pseudo-nitzschia subcurvata* in a 6 day competition

636 experiment with *Phaeocystis antarctica* at 0°C and 6°C. The competition experiments were

637 started with equal Chl *a* concentrations for both species, and the relative abundance was

638 calculated based on cell counts. Values represent the means and error bars represents the

639 standard deviations of triplicate samples.

640

641 Fig. 5. CO_2 functional response curves showing specific growth rates (and fitted curves) across a

642 range of CO_2 concentrations from ~100 ppm to ~1730 ppm at 2°C and at 8°C. *Pseudo-nitzschia*

643 *subcurvata* at 2°C (A) and 8°C (B) and *Phaeocystis antarctica* at 2°C (C) and 8°C (D). Values

644 represent the means and error bars represents the standard deviations of triplicate samples.

645
646
647

648   Fig. 1
649
650
651
652
653
654
655
656
657
658
659
660
661
662
663
664
665
666
667
668
669
670
671
672
673
674
675
676
677
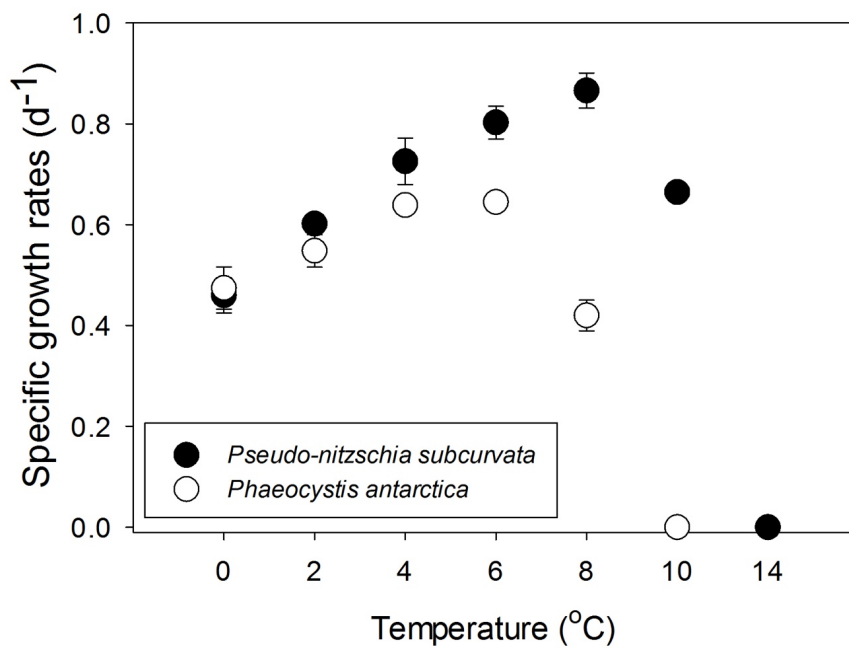
678   Fig. 2
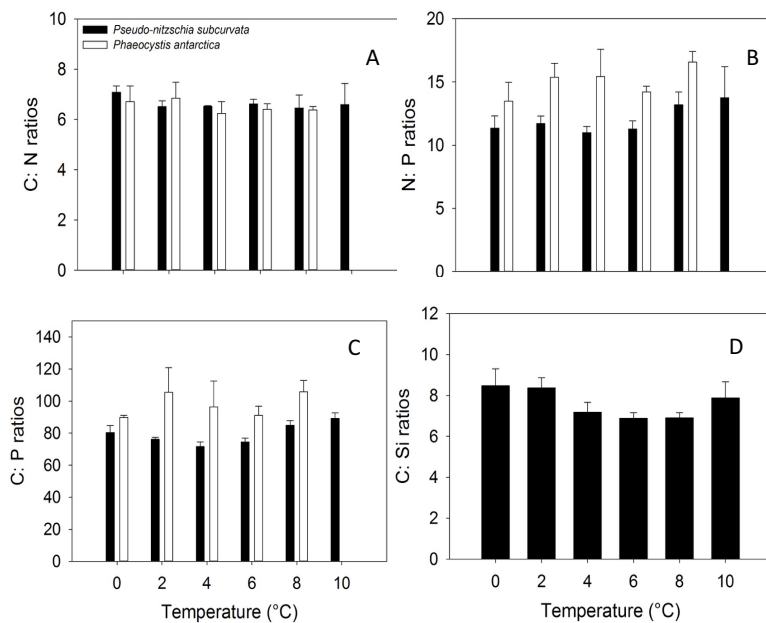
720   Fig. 3
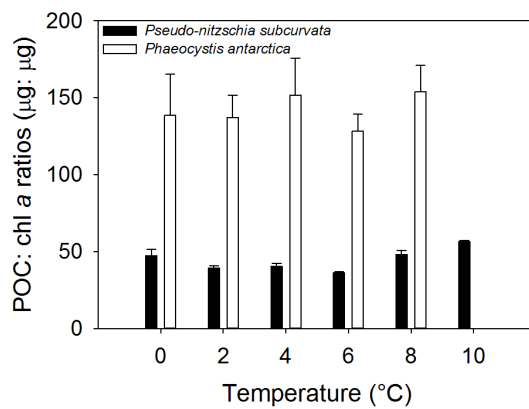
721   Fig. 4
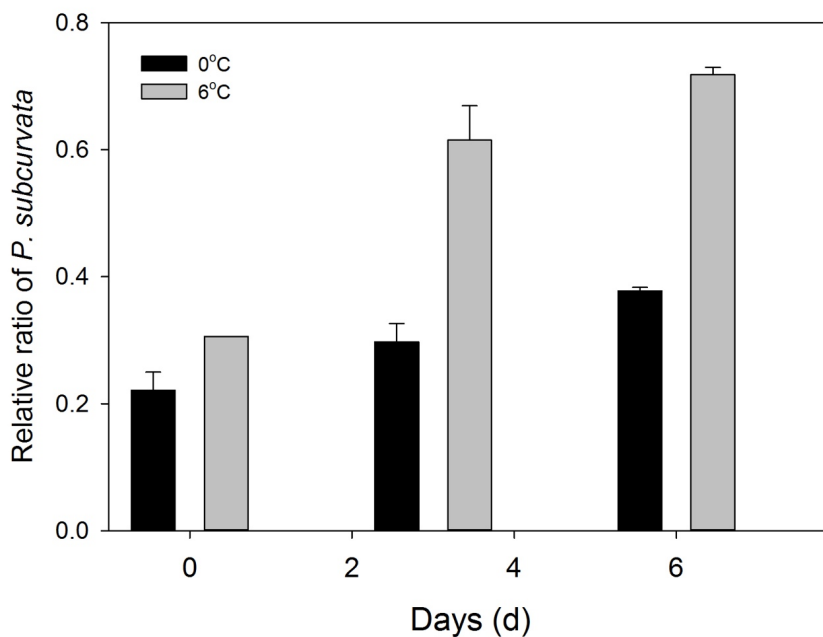
746   Fig. 5
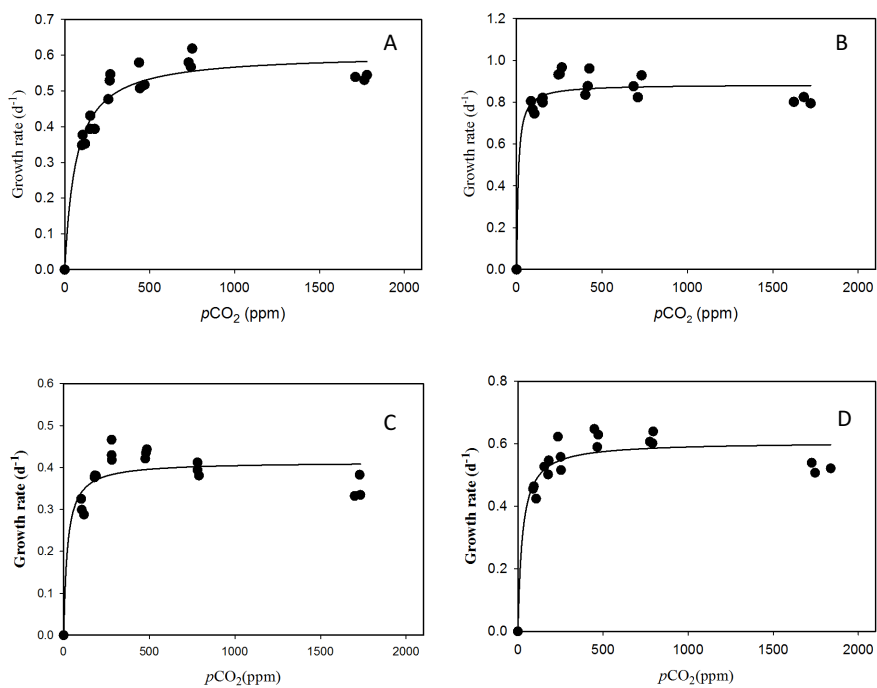
747
748
749
750
751
752
753
754
755
756
757
758
759
760
761
762
763
764
765
766
767
768
769
770